

Dynamic properties of a building with viscous dampers in non-proportional arrangement

Luis E. Suarez*¹ and Carlos A. Gaviria^{1,2a}

¹*Department of Civil Engineering and Surveying, University of Puerto Rico at Mayaguez,
Mayaguez, 00681-9000, Puerto Rico*

²*Civil Engineering Program, Universidad de la Costa, Barranquilla, Colombia*

(Received January 1, 2015, Revised August 9, 2015, Accepted September 15, 2015)

Abstract. Any rational approach to define the configuration and size of viscous fluid dampers in a structure should be based on the dynamic properties of the system with the dampers. In this paper we propose an alternative representation of the complex eigenvalues of multi degree of freedom systems with dampers to calculate new equivalent natural frequencies. Analytical expressions for the dynamic properties of a two-story building model with a linear viscous damper in the first floor (i.e. with a non-proportional damping matrix) are derived. The formulas permit to obtain the equivalent damping ratios and equivalent natural frequencies for all the modes as a function of the mass, stiffness and damping coefficient for underdamped and overdamped systems. It is shown that the commonly used formula to define the equivalent natural frequency is not applicable for this type of system and for others where the damping matrix is not proportional to the mass matrix, stiffness matrix or both. Moreover, the new expressions for the equivalent natural frequencies expose a novel phenomenon; the use of viscous fluid dampers can modify the vibration frequencies of the structure. The significance of the new equivalent natural frequencies is expounded by means of a simulated free vibration test. The proposed approach may offer a new perspective to study the effect of viscous dampers on the dynamic properties of a structure.

Keywords: equivalent frequencies; damping ratios; dampers; state equations; complex eigenvalues

1. Introduction

Viscous fluid dampers are one of the most popular alternatives among the currently available passive seismic protection devices. They are relatively economical, easy to install, efficient, and invasiveness issues can be minimized. These devices can be attached to a new or existing structure and its applications experienced a rapid growth since the mid-1990s (Symans *et al.* 2008). Some studies demonstrated that viscous fluid dampers are the second most efficient passive protective system in terms of response reduction, after seismic base isolation (Mayes and Naguib 2005).

The design of a system of viscous fluid dampers for a specific structure involves the selection of the sizes and locations of the dampers, and thus several methods were proposed to determine

*Corresponding author, Professor, E-mail: luis.suarez3@upr.edu

^aFormer Ph.D. Student

the optimal location of the dampers in a structure (Pettinga *et al.* 2013). For example, a comprehensive comparison of five methods for optimal placement of viscous dampers is presented by Whittle *et al.* (2012). However, when optimal damper systems are sought, usually only dampers localized between adjacent floors are considered, and other arrangements technically and physically implementable did not receive the same attention (Trombetti and Silvestri 2006).

With regard to the size of the dampers, the manufacturers usually recommend that the dampers should be such that the fundamental mode (the first mode for buildings subjected to seismic or wind loads) has a 25% damping ratio as a practical upper limit (Lee and Taylor 2001). In practice and for several reasons (lack of familiarity with the theories, inadequate computer programs, etc.) the selection of the size and position is frequently done by trial and error. For instance, the structure with dampers is modeled with structural engineering software and the seismic response under different earthquake scenarios is obtained until the designer is satisfied with the results. Thus, target damping ratios attained for the dominant modes and the change in frequencies are not taken into account, at least in the initial stages of the design.

A more rational method for the design of a system of linear viscous dampers is estimating the damping level achieved for a specific position and size of the dampers. Several researchers proposed approaches to accomplish this goal (e.g., Constantinou and Symans 1993, Soong and Dargush 1997, Occhiuzzi 2009, Pierson *et al.* 2013). The method is based on rewriting the equations of motion of the structure with dampers in the state space form (Antsaklis and Michel 2007) and from the eigenvalue analysis associated with free vibrations one can obtain accurate information on equivalent natural frequencies and damping ratios for all the modes of interest (Charney and McNamara 2008).

There are situations where the state space approach is not applicable. This is the case for dampers in which the damping forces are a function of the velocity elevated to an exponent less than 1. Another example is when the seismic force-resisting system undergoes inelastic deformations during a strong earthquake event (Cheng *et al.* 2010). Nevertheless, even in these cases a linear analysis is usually done to begin the design process. This type of linear analysis but using energy-based and optimization approaches was also used in recent studies to determine the optimal damper locations (Lewandowski 2008, Lin *et al.* 2013).

A noteworthy application of the state space approach was presented by Trombetti and Silvestri (2006, 2007). They investigated the modal damping ratios of shear-type buildings, characterized by constant lateral stiffness and floor mass, and equipped with viscous dampers in a Rayleigh damping disposition, i.e. the dampers were installed in a mass proportional damping (MPD) or stiffness proportional damping (SPD) configuration. The results show that the first modal damping ratio of a structure with the MPD system is always larger than the first modal damping ratio of a structure with the SPD system. Morzfeld *et al.* (2009) studied the non-classically damped systems ignoring the off-diagonal elements of the modal damping matrix. Via numerical examples it was shown that the error due to the decoupling approximation increases monotonically while the modal damping matrix becomes more diagonally dominant. Ma *et al.* (2010) used a previously developed method called phase synchronization (Ma *et al.* 2009) to decouple viscously damped linear system in non-oscillatory free vibration and in forced vibration. They proposed and validated a general methodology that requires the solution of a quadratic eigenvalue problem. Charney and McNamara (2008) compared the modal strain energy method using the undamped mode shapes, free vibration log decrement, and complex eigenvalue-eigenvector analysis for determining the equivalent viscous damping ratios in a linear-elastic one-story shear building model. The modal strain energy approach consistently yielded increasing effective damping with increased damper size, while the

other two methods predicted the opposite results. As an alternative to state-space based approaches, Adhikari (2011) proposed an iterative method to obtain the eigenvalues and eigenvectors of nonproportionally damped systems based on the undamped eigenproperties. The method needs to satisfy a sufficient condition for its convergence and due to its iterative nature is limited to numerical analysis. More recently, Lewandowski and Pawlak (2011) studied the dynamic response of frames with viscoelastic dampers (VE) modeled with the fractional derivative Kelvin and Maxwell models. They proposed a new state space formulation to write the equations of motions and an associated nonlinear eigenvalue problem was solved with the continuation method. In a following paper Lewandowski *et al.* (2012) compared the dynamic properties of frames equipped with VE dampers represented with classical rheological models, a fractional order derivative model, and the complex modulus approach. The dynamic behavior predicted by each approach was compared in the frequency domain. The dynamic characteristics of structures with VE dampers are further studied by Pawlak and Lewandowski (2013). The dynamic behavior of these structures is characterized by the natural frequencies and damping factors which are determined from a nonlinear eigenvalue problem. The nonlinear eigenvalue problem is solved using the continuation method. Although the dimension of the eigenvalue problem is the same for a structure with and without dampers, it requires an incremental-iterative procedure for its solution. In a following paper Pawlak and Lewandowski (2014) evaluated the qualitative differences in the dynamic characteristics of a system equipped with dampers modeled with the Kelvin and fractional models. For a two story shear frame they found that the non-dimensional damping ratios are limited for several or all modes of vibration whereas bifurcation point in the frequencies of the system takes place. The previous conclusion is in agreement with the results reported by Krenk (2005) for a viscous tuned mass damper. He used the classical dynamic amplification analysis considering the dynamic amplitude of the relative motion of the damper. Krenk demonstrated that for the classic tuning of the damper frequency, the complex locus of the natural frequencies has a bifurcation point corresponding to maximum damping of the modes.

Despite of the valuable aforementioned studies, an analytical investigation of the fundamental dynamic properties (i.e. equivalent natural frequencies and damping ratios) of shear-type buildings with a non-proportional damper arrangement is not available. This is important because most real structures with added viscous fluid dampers are not proportionally damped (Charney and McNamara 2008), i.e., the dampers are reduced in size or suppressed in the upper floors (e.g., Lewandowski 2008, Miyamoto and Gilani 2008).

This paper is a first step in the quest for an analytical and rational framework to select the non-proportional damper configuration and size based on the properties of the structure. Because of the complicated algebraic nature of the problem, the procedure is presented for a regular 2-story building with a single damper in the lower floor. Closed form formulas that permit to define the equivalent natural frequencies and damping ratios are derived. The structure is modeled as a linear elastic shear building and the dampers are assumed to have a linear, purely viscous behavior. The equations derived permit to determine in closed form the damping ratios that can be attained for each mode for a given value of the damping coefficient and structural properties. Very interesting and so far unreported phenomena occur when the variation of the dynamic properties with the damping coefficient are studied. It is shown that the usual definitions of the equivalent damping ratios and natural frequencies (Soong and Dargush 1997, Occhiuzzi 2009) do not apply for this case and a new way to characterize the complex eigenvalues of damped multi degree of freedom system is proposed. The case of overdamped systems is also studied. The physical interpretation of the equivalent natural frequencies is discussed. Also, the implications in the seismic response are

presented by means of a simple numerical example.

2. Free vibration response of non-classically damped linear systems

A brief introduction to the analysis of non-classically damped linear systems will be presented. Although this is not the object of this paper, it is necessary to understand the concepts and formulation presented later.

We are interested in solving the following equations of motion of a structure with viscous fluid dampers and n degrees of freedom in free vibration

$$[M]\{\ddot{u}\} + [C]\{\dot{u}\} + [K]\{u\} = \{0\} \quad (1)$$

where $[M]$ and $[K]$ are, respectively, the mass and stiffness matrices, and $[C]$ is the real, symmetric damping matrix formed by assembling the coefficients of the viscous dampers. It is well known that because of the presence of the matrix $[C]$, the Eq. (1) cannot be decoupled with the conventional (real) modes of vibration (Pawlak and Lewandowski 2013). An exception occurs when the damping matrix is a linear combination of the mass and/or stiffness matrix, and thus the system is classically damped (Humar 2012). To solve the equations with the modal analysis technique, it is necessary to rewrite the equations of motion in state space form, i.e. as a system of $2n$ first order differential equations (Constantinou and Symans 1993, Veletsos and Ventura 1986, Antsaklis and Michel 2007, Charney and McNamara 2008)

$$\{\dot{z}\} = [A]\{z\} \quad \therefore \quad \begin{Bmatrix} \{\dot{u}\} \\ \{\dot{u}\} \end{Bmatrix} = \begin{bmatrix} -[M]^{-1}[C] & -[M]^{-1}[K] \\ [I] & [0] \end{bmatrix} \begin{Bmatrix} \{u\} \\ \{u\} \end{Bmatrix} \quad (2)$$

where $\{z\}$ and $[A]$ are the state vector and the non-symmetric system matrix, respectively. Eq. (2) is not the only way to express the equations of motion in state space form. However, they are all equivalent and we selected the simplest one.

To decouple the equations of motion in the state space form we need to solve the associated eigenvalue problem

$$[A]\{\psi\}_j = \lambda_j \{\psi\}_j \quad ; \quad j = 1, 2, \dots, 2n \quad (3)$$

where the eigenvectors $\{\psi\}_j$ and eigenvalues λ_j are, in general, complex quantities, but as the damping in the system increases they could also be real. If the eigenproperties are complex, they occur in complex conjugate pairs, and if they are real there is always an even number of them.

Introducing in Eq. (2) the coordinate transformation $\{z\} = [\Psi]\{\eta\}$ where $[\Psi]$ is the matrix with $2n$ eigenvectors $\{\psi\}_j$, and premultiplying by its inverse one obtains a set of $2n$ decoupled first order ordinary differential equations. By this transformation, the state vector (Eq. (2)) in terms of real quantities is obtained as

$$\begin{Bmatrix} \{\dot{u}\} \\ \{u\} \end{Bmatrix} = \sum_{j=1}^{2n} \left(\{A_j\} \cos \omega_{d,j} t + \{B_j\} \sin \omega_{d,j} t \right) e^{-\xi_j \omega_j t} \quad (4)$$

where $\{A_j\}$ and $\{B_j\}$ are vectors with real constants, $\omega_{d,j} = \omega_j \sqrt{1 - \xi_j^2}$, ω_j and ξ_j are, respectively, the damped equivalent natural frequency, the equivalent natural frequency and the equivalent modal

damping ratio of the j^{th} mode. Furthermore, Eq. (4) can be written in a form similar to the expression that defines the response of classically damped systems. In order to do this, the following crucial assumption is done. Following the theory of the response of a damped single degree of freedom system, the complex eigenvalue is expressed as

$$\lambda_j = -\xi_j \omega_j + i \omega_j \sqrt{1 - \xi_j^2} \tag{5}$$

It is easy to verify that the equivalent frequencies and modal damping ratios are

$$\omega_j = |\lambda_j| \tag{6a}$$

$$\xi_j = -\text{Real}(\lambda_j) / |\lambda_j| \tag{6b}$$

More details about the state space representation can be found in Constantinou and Symans (1993).

3. The eigenvalue problem of a building model with a single damper

We will now consider a 2-story regular building modeled as a shear building with one degree of freedom per floor (Suarez and Gaviria 2014). The shear building model under study is shown in Fig. 1(a). The mass lumped at each of the two floors is m , the total lateral stiffness of each story is k and the damper coefficient of the viscous dashpot at the first floor is c . The equations of motion (Eq. (1)) of this multi degree of freedom system (mdof) in free vibrations are

$$\begin{bmatrix} m & 0 \\ 0 & m \end{bmatrix} \begin{Bmatrix} \ddot{u}_1 \\ \ddot{u}_2 \end{Bmatrix} + \begin{bmatrix} c & 0 \\ 0 & 0 \end{bmatrix} \begin{Bmatrix} \dot{u}_1 \\ \dot{u}_2 \end{Bmatrix} + \begin{bmatrix} 2k & -k \\ -k & k \end{bmatrix} \begin{Bmatrix} u_1 \\ u_2 \end{Bmatrix} = \begin{Bmatrix} 0 \\ 0 \end{Bmatrix} \tag{7}$$

where u_1 and u_2 are the lateral displacements of the floors. By solving the associate eigenvalue problem of the undamped system, we can obtain the undamped natural frequencies

$$\omega_{n1} = (\sqrt{5} - 1)\Omega / 2 = 0.618\Omega \quad ; \quad \omega_{n2} = (\sqrt{5} + 1)\Omega / 2 = 1.618\Omega \tag{8}$$

where Ω is a frequency parameter equal to the natural frequency of a single degree of freedom system (sdof) with the same mass and lateral stiffness of one floor

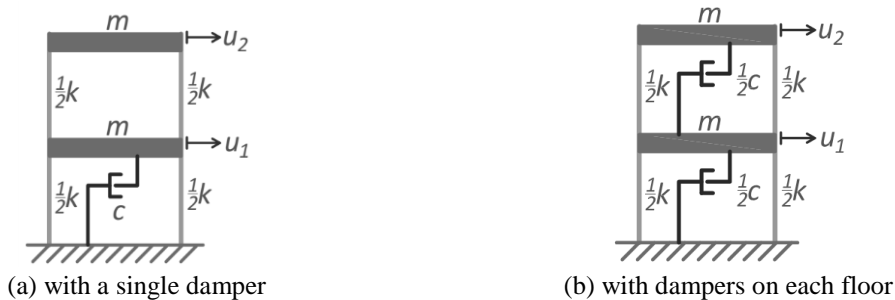


Fig. 1 Two-story shear building model

$$\Omega = \sqrt{(k/m)} \quad (9)$$

We are interested in the eigenproperties of the damped structural system. To obtain the complex eigenvalues λ_j and modes of vibration $\{\psi\}_j$ the equations of motion are rewritten in state space form and the associated eigenvalue problem is formed. To simplify the ensuing equations it is convenient to introduce a dimensionless damping coefficient x defined as follows

$$x = c/\sqrt{km} = c/(\Omega m) \quad (10)$$

It can be shown that the eigenvalue problem in Eq. (3) can now be written as

$$\begin{bmatrix} -x\Omega - \lambda_j & 0 & -2\Omega^2 & \Omega^2 \\ 0 & -\lambda_j & \Omega^2 & -\Omega^2 \\ 1 & 0 & -\lambda_j & 0 \\ 0 & 1 & 0 & -\lambda_j \end{bmatrix} \begin{Bmatrix} \psi_{1j} \\ \psi_{2j} \\ \psi_{3j} \\ \psi_{4j} \end{Bmatrix} = \begin{Bmatrix} 0 \\ 0 \\ 0 \\ 0 \end{Bmatrix} \quad (11)$$

and its fourth order characteristic polynomial associated with the eigenvalue problem is (Suarez and Gaviria 2014)

$$p(\lambda) = (\lambda/\Omega)^4 + x(\lambda/\Omega)^3 + 3(\lambda/\Omega)^2 + x(\lambda/\Omega) + 1 \quad (12)$$

The roots of the characteristic polynomial can be found in closed form using the computer algebra system Mathematica (Wolfram 2012)

$$\hat{\lambda}_1 = -\left(x + \sqrt{x^2 - 4} \pm \sqrt{2}\sqrt{x^2 - 10 + x\sqrt{x^2 - 4}}\right)\Omega/4 \quad (13a)$$

$$\hat{\lambda}_3 = -\left(x - \sqrt{x^2 - 4} \pm \sqrt{2}\sqrt{x^2 - 10 - x\sqrt{x^2 - 4}}\right)\Omega/4 \quad (13b)$$

The magnitudes of the eigenvalues in non-dimensional form, $|\hat{\lambda}_i|/\Omega$, are plotted in Fig. 2(a).

The eigenvalues plotted in Fig. 2(a) show that once x reaches a value of 2, the moduli of all the eigenvalues become for a certain range of x . The value of the non-dimensional coefficient $x=2$ is associated to a particular damping coefficient c_{c1} , which will be denoted as the ‘‘first critical damping coefficient’’ and is defined in Eq. (14a). The fact that all eigenvalues converge to the same absolute value $|\lambda_i|=\Omega$ is an unusual and interesting phenomenon in its own right, but its discussion will be postponed for now. The absolute value of the eigenvalues remains constant between the values of $x=2$ (the first critical damping coefficient) and $x=2.5$. The latter value of x corresponds to a value of $c=c_{c2}$ and it will be referred to as the ‘‘second critical damping coefficient’’ defined in Eq. (14b).

$$c_{c1} = 2\Omega m = 2\sqrt{km} \quad (14a)$$

$$c_{c2} = 2.5\Omega m = 2.5\sqrt{km} \quad (14b)$$

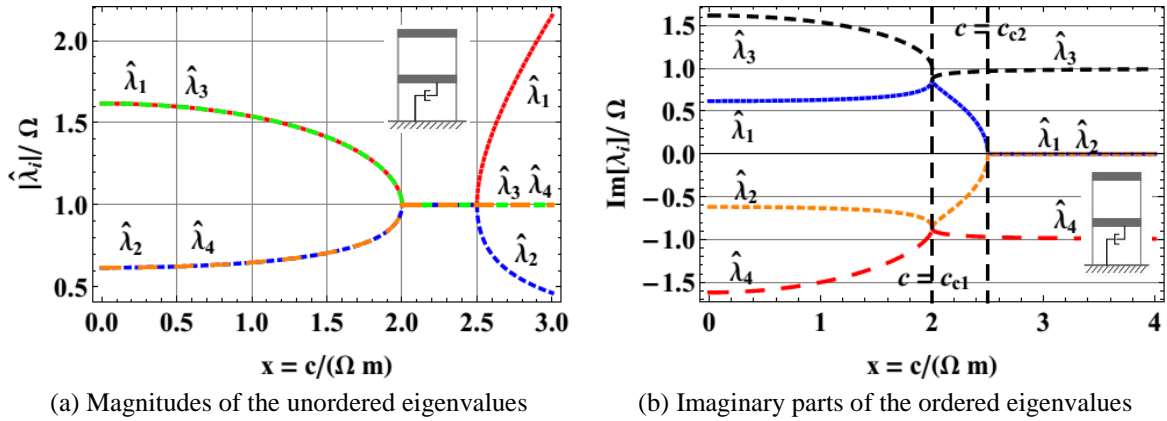


Fig. 2 Variation of eigenvalues

It is called attention to the fact that the eigenvalues shown in Fig. 2(a) are not in any specific order, which is a potential shortcoming to carry out modal analysis. The ordering of the eigenvalues is a trivial issue for undamped systems because they are all real and positive and thus they are sorted in ascending order. Nevertheless, in the case of damped structural systems, the eigenvalues are complex (when their associated modes are underdamped, otherwise they become real). After trying with several schemes, it was decided to order the eigenvalues according to the absolute value of the imaginary parts, i.e., $|\text{Im}(\lambda_1)| < |\text{Im}(\lambda_2)| < |\text{Im}(\lambda_3)| < |\text{Im}(\lambda_4)|$. For a complex conjugate pair, the eigenvalue with the negative imaginary part was ordered after the one with the positive part. Fig. 2(b) shows the imaginary parts of the ordered eigenvalues in non-dimensional form, i.e., $|\text{Im}(\lambda_i)|/\Omega$. As it was expected, the figure shows that initially the pair $\text{Im}(\lambda_1)/\Omega$ and $\text{Im}(\lambda_2)/\Omega$, and the pair $\text{Im}(\lambda_3)/\Omega$ and $\text{Im}(\lambda_4)/\Omega$ have equal magnitudes but opposite signs. However, after a value of $x=2.5$ (i.e., for $c \geq c_{c2}$), the imaginary parts of λ_1 and λ_2 become zero implying that the corresponding modes become overdamped, as it is evident from Eq. (5) for $\zeta_j \geq 1$.

For comparison purposes, a shear building with a stiffness proportional damping system is considered (see Fig. 1(b)). The building has two dampers with coefficients $c/2$ on each of the two floors (so that the sum of the two damping coefficients is equal to c of the building with one damper). Fig. 3(a) shows the variation of the equivalent natural frequencies (i.e., the modulus of the eigenvalues) as a function of the dimensionless damping coefficient x . It can be seen that the moduli of all the eigenvalues remain constant while the modes are underdamped. The eigenvalue of the first mode λ_1 and its complex conjugate λ_2 are underdamped regardless of the value of c , whereas the moduli of the second mode eigenvalue λ_3 and its complex conjugate λ_4 diverge when the mode becomes overdamped (and the eigenvalues become real).

3.1 Closed form of the complex eigenvalues

Fig. 2(b) permits to identify the correct sequence of the eigenvalues presented in Eqs. (13) obtained from the roots of the characteristic polynomial. Eqs. (15a)-(15g) display the expressions for the ordered eigenvalues. In most cases the eigenvalues must be defined by two different expressions depending on the value of the parameter x (or equivalently the damping coefficient c). The only exception is the first eigenvalue which is defined by a single expression (Eq. (15a)).

$$\lambda_1 = -\left(x + \sqrt{x^2 - 4} - \sqrt{2}\sqrt{x^2 - 10 + x\sqrt{x^2 - 4}}\right)\Omega/4 \quad ; \quad \text{for all } c \quad (15a)$$

$$\lambda_2 = -\left(x - \sqrt{x^2 - 4} - \sqrt{2}\sqrt{x^2 - 10 - x\sqrt{x^2 - 4}}\right)\Omega/4 \quad ; \quad c \leq c_{c1} \quad (15b)$$

$$\lambda_2 = -\left(x + \sqrt{x^2 - 4} + \sqrt{2}\sqrt{x^2 - 10 + x\sqrt{x^2 - 4}}\right)\Omega/4 \quad ; \quad c > c_{c1} \quad (15c)$$

$$\lambda_3 = -\left(x - \sqrt{x^2 - 4} + \sqrt{2}\sqrt{x^2 - 10 - x\sqrt{x^2 - 4}}\right)\Omega/4 \quad ; \quad c \leq c_{cc1} \quad (15d)$$

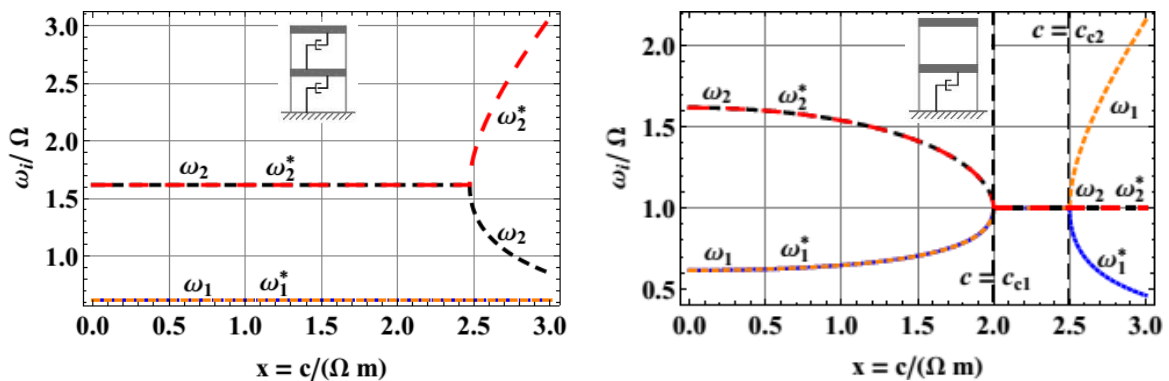
$$\lambda_3 = -\left(x - \sqrt{x^2 - 4} - \sqrt{2}\sqrt{x^2 - 10 - x\sqrt{x^2 - 4}}\right)\Omega/4 \quad ; \quad c > c_{c1} \quad (15e)$$

$$\lambda_4 = -\left(x + \sqrt{x^2 - 4} + \sqrt{2}\sqrt{x^2 - 10 + x\sqrt{x^2 - 4}}\right)\Omega/4 \quad ; \quad c \leq c_{c1} \quad (15f)$$

$$\lambda_4 = -\left(x - \sqrt{x^2 - 4} + \sqrt{2}\sqrt{x^2 - 10 - x\sqrt{x^2 - 4}}\right)\Omega/4 \quad ; \quad c > c_{c1} \quad (15g)$$

4. Variation of the equivalent natural frequencies with the damping coefficient

It was shown in Fig. 2(a) how the magnitudes of the complex eigenvalues change with the damping coefficient for the case of a building with a single damper. On the other hand, Fig. 3(a) corroborated that for a building with a damper on each story, the equivalent natural frequencies (i.e., the magnitudes $|\lambda_{i}|$) remain constant until the modes become overdamped.



(a) A building with equal dampers in the two floors (b) A building with single dampers at the first floor

Fig. 3 Equivalent natural frequencies

It is also interesting to examine how the equivalent natural frequencies vary with the damping coefficient. The equivalent natural frequencies were defined in Eq. (6a) as the absolute values (or moduli) of the eigenvalue, i.e., $\omega_1 = |\lambda_1|$; $\omega_1^* = |\lambda_2|$; $\omega_2 = |\lambda_3|$; $\omega_2^* = |\lambda_4|$, where ω_1^* and ω_2^* denote the frequencies from the complex conjugate eigenvalues. Fig. 3(b) depicts the variation of the equivalent natural frequencies in non-dimensional form ω_i/Ω with the dimensionless damping coefficient x . This figure is similar to Fig. 2(a) but now the ordered eigenvalues given by Eqs. (15a)-(15g) are used. It can be seen that while the modes are underdamped, ω_1^* and ω_2^* are equal to ω_1 and ω_2 , respectively.

The behavior of the equivalent natural frequencies displayed in Fig. 3(b) is unexpected. For instance, according to Eqs. (5) and (6a) ω_1 should be constant and equal the first undamped natural frequency designated as ω_{n1} in Eq. (8). That is, it was expected that the first natural frequency would be

$$\omega_1 = |\lambda_1| = \sqrt{(\xi_1 \omega_{n1})^2 + (\omega_{n1} \sqrt{1 - \xi_1^2})^2} = \omega_{n1} \tag{16}$$

However, according to Fig. 3(b) the equivalent natural frequency ω_1 (and ω_1^*) is equal to the undamped natural frequency only for $x=0$ (i.e., $c=0$) and then starts increasing until $x=2$ (i.e., $c=c_{c1}$). We can then conclude that Eq. (16) is never valid. Also in the zone $0 < x \leq 2$ the natural frequency ω_2 (and ω_2^*) decreases as x (or c) increases. The incongruity arises because the assumption that led to Eq. (5) does not always hold. Probably the equation stemmed from the case of a building with dampers in all floors, where it is always applicable as long as ξ_j is less than 1. This can be clearly seen in Fig. 3(a), which shows that the moduli of the eigenvalues (or equivalent natural frequencies) of the building with two dampers are equal to the undamped frequencies while the modes are underdamped.

Going back to the behavior of the equivalent natural frequencies depicted in Fig. 3(b), note that when the damping coefficient c reaches c_{c1} ($x=2$), the equivalent frequencies attain a plateau. The imaginary parts of the eigenvalues are not zero yet (see Fig. 3) meaning that the equivalent damping ratios are still less than 1. In the region $2 \leq x \leq 2.5$, or in terms of the damping coefficient when $c_{c1} \leq c \leq c_{c2}$, all the equivalent natural frequencies fuse into a single frequency Ω

$$\Omega = \omega_1 = \omega_1^* = \omega_2 = \omega_2^* = \sqrt{k/m} \quad ; \quad c_{c1} \leq c \leq c_{c2} \tag{17}$$

For values of $c > c_{c2}$, the frequency ω_1 starts to decrease and ω_1^* grows as $c \rightarrow \infty$. For these values of c , the first mode is overdamped (the damping ratios will be examined in a following section). Moreover, as it is discussed later, the definition of equivalent natural frequency based on the combination of Eqs. (5) and (6) cannot be applied in this region. As a matter of fact, for an overdamped system the concept of equivalent natural frequency is not applicable, since the structure will not oscillate when given initial conditions and set in free vibrations. This issue will be further discussed in a following section. Also, note that there are no changes in the behavior of ω_2 and ω_2^* when $c > c_{c2}$: they remain constant and equal to Ω .

4.1 An alternative way to represent the complex eigenvalues

It was shown in the previous section that Eq. (5) is not always valid, at least for buildings without dampers uniformly distributed in all floors. To circumvent this problem, we propose the following more general expression to represent the complex eigenvalues, instead of the classical

form in Eq. (5)

$$\lambda_j = -\xi_j |\lambda_j| + i |\lambda_j| \sqrt{1 - \xi_j^2} \quad ; \quad j = 1, 2, \dots, 2n \quad (18)$$

Eq. (5) is now a special case of Eq. (18) and it is easy to verify that the definitions of the equivalent frequencies (Eq. (6a)) and modal damping ratios (Eq. (6b)) are still valid. Moreover, this definition is valid for any mdof system and the response of system can still be obtained with Eq. (4). However, it is important to call attention to the fact that the frequency ω_j in Eq. (4) should not be the undamped natural frequency but rather the equivalent frequency equal to $|\lambda_j|$. The implications and physical meaning of the new equivalent natural frequency ($\omega_{i=|\lambda_i|}$) will be given later.

4.2 Analytical expressions of the equivalent natural frequencies of underdamped systems

It would be interesting and useful to have closed form expressions for the equivalent frequencies in terms of the properties of the structural system. To do this, we need to identify the real and imaginary parts of the expressions in Eq. (15). In particular, the real parts are useful to define the equivalent damping ratios in closed form.

We will begin by examining the first eigenvalue. Although the complex eigenvalue λ_1 is defined by Eq. (15a), it is not evident which parts of these expressions define the real and imaginary parts. To reveal them, we begin by rewriting λ_1 in Eq. (15a) as

$$\lambda_1 = -\left(x + i\sqrt{a} - \sqrt{2i}\sqrt{b + ix\sqrt{a}}\right)\Omega/4 \quad (19)$$

where $a=4-x^2$ and $b=x^2-10$ are real-valued constants. Also, the complex number $b + ix\sqrt{a}$ in the third square root in Eq. (19) can be written in polar form as $|z| e^{i\theta}$ with the modulus and phase angle respectively given by: $|z| = \sqrt{b^2 + x^2a}$ and $\theta = \tan^{-1}(x\sqrt{a}/b)$. With this notation the complex eigenvalue becomes

$$\lambda_1 = -\left[x + \sqrt{2}\sqrt{\sqrt{b^2 + x^2a}} \sin \frac{\theta}{2} + i\left(\sqrt{a} - \sqrt{2}\sqrt{\sqrt{b^2 + x^2a}} \cos \frac{\theta}{2}\right)\right]\Omega/4 \quad (20)$$

Substituting back the constants a and b , and using Eq. (6a), the analytical expression of the first equivalent natural frequency ω_1 can be written as

$$\omega_1 = \omega_1^* = \frac{\Omega}{2} \sqrt{1 + \sqrt{25 - 4x^2} + (25 - 4x^2)^{1/4} \left(x \sin \phi - \sqrt{4 - x^2} \cos \phi\right)} \quad ; \quad c \leq c_{c1} \quad (21a)$$

where $\phi = 0.5 \tan^{-1}\left(x\sqrt{4-x^2}/x^2-10\right)$. Note that in the region $c \leq c_1$ considered, the natural frequencies ω_1 and ω_1^* are equal (see Fig. 3(b)). In the range $c_{c1} \leq c \leq c_{c2}$ the values of ω_1 and ω_1^* are defined by Eq. (17).

Turning the attention to the eigenvalue of the second mode, denoted as λ_3 , it is recalled that it is defined by two expressions, Eqs. (15d) and (15e), depending on the value of c . The expression derived will be valid in the first region (i.e., $c \leq c_{c1}$). Following a procedure similar to that applied to

λ_1 , it can be shown that the second equivalent frequency ω_2 (and ω_2^*) can be defined as follows

$$\omega_2 = \omega_2^* = \frac{\Omega}{2} \sqrt{1 + \sqrt{25 - 4x^2} - (25 - 4x^2)^{1/4} (x \sin \phi - \sqrt{4 - x^2} \cos \phi)} \quad ; \quad c \leq c_{c1} \quad (21b)$$

Here again in the range $c_{c1} \leq c \leq c_{c2}$ the values of ω_2 and ω_2^* are defined by Eq. (17).

Although the values of the first c_{c1} and second critical damping coefficient c_{c2} specified in Eqs. (14a) and (14b) were obtained by examining Fig. 2, they can be defined in an analytical way. This can be done by noticing from Fig. 2(b) that when the damping coefficient is equal to the first critical value ($c=c_{c1}$ or $x=2$), the imaginary parts $\text{Im}(\lambda_1)$ and $\text{Im}(\lambda_3)$ are equal. The imaginary part of λ_1 is given in Eq. (20) and there is a corresponding expression for λ_3 . Subtracting the imaginary parts of λ_1 and λ_3 , equating the resulting expression to zero, and solving for x leads to

$$\text{Im}(\lambda_1) - \text{Im}(\lambda_3) = -\frac{\Omega}{2} \sqrt{4 - x^2} = 0 \quad \therefore \quad x = 2 \quad (22)$$

which means that the first critical damping coefficient is $c_{c1} = 2\sqrt{km}$.

To verify the value of the damping coefficient c_{c2} at the end of the second region (i.e., the zone where all the equivalent natural frequencies are equal) we can make use of the fact that the imaginary part of λ_1 (and λ_2) becomes zero there (see Fig. 3). Examining the expression for the first eigenvalue in Eq. (15a) for the case where $x > 2$ ($c > c_{c1}$), it is possible to identify the imaginary part of the eigenvalue λ_1 . Setting this imaginary part to zero and solving for x we obtain

$$x^2 - 10 + x\sqrt{x^2 - 4} = 0 \quad \Rightarrow \quad x = 2.5 \quad (23)$$

and therefore the second critical damping coefficient is $c_{c2} = 2.5\sqrt{km}$.

5. Analytical expressions for the equivalent damping ratios

It was mentioned that with the proposed Eq. (18) to characterize the eigenvalues, Eq. (6b) can still be used to calculate the modal damping ratios. In theory, the damping ratios in the first region ($c \leq c_{c1}$) can be calculated by simply substituting Eq. (15a) or Eq. (15b) and Eq. (15d) or Eq. (15f) in Eq. (6b). Although this will yield an exact closed form expression, the resulting formula is too complicated to be useful. Therefore, as an alternative the following approximate expression is proposed

$$\xi_1 = \xi_2 \approx 0.2236x + 0.0045x^3 \quad ; \quad c \leq c_{c1} \quad (24)$$

The formula was obtained by applying a Taylor series expansion to the exact expression around $c=0$. To verify its accuracy, Eq. (24) is compared in Fig. 4 (continuous line) with the exact closed form expression (dashed line).

The equivalent damping ratios ζ_1 and ζ_2 for $c > c_{c1}$ can be obtained by replacing Eqs. (15c) and (15e) in Eq. (6b). The resulting expressions are given in Eqs. (25a) and (25b). Note that the range of application of Eq. (25a) is different from Eq. (25b). This is so because when $c > c_{c2}$ the imaginary part of λ_1 (and λ_2) is zero (see Fig. 3), and thus the first mode is overdamped and Eq. (6b) will always yield 1. Therefore, Eq. (25a) is only valid in the second region ($c_{c1} < c < c_{c2}$). On the other hand, the eigenvalue λ_3 (and λ_4) remains complex when $c > c_{c2}$ (see Fig. 2(b)) and thus Eq. (25b) is

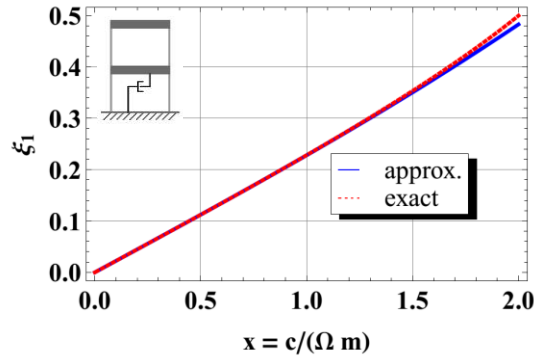


Fig. 4 Comparison between the exact and approximate damping ratio for the 1st mode

also valid in this third region while $\zeta_2 \leq 1$.

$$\xi_1 = \left(x + \sqrt{x^2 - 4} \right) / 4 \quad ; \quad c_{c1} < c \leq c_{c2} \tag{25a}$$

$$\xi_2 = \left(x - \sqrt{x^2 - 4} \right) / 4 \quad ; \quad c > c_{c1} \tag{25b}$$

To obtain the damping ratio for the first mode in the third region (i.e., where $c \geq c_{c2}$), we propose to write the pair of real eigenvalues λ_r and λ_{r+1} of the r^{th} and $(r+1)^{th}$ modes as

$$\lambda_r = -\xi_r \Omega_r + \Omega_r \sqrt{\xi_r^2 - 1} \quad ; \quad \lambda_{r+1} = -\xi_r \Omega_r - \Omega_r \sqrt{\xi_r^2 - 1} \tag{26}$$

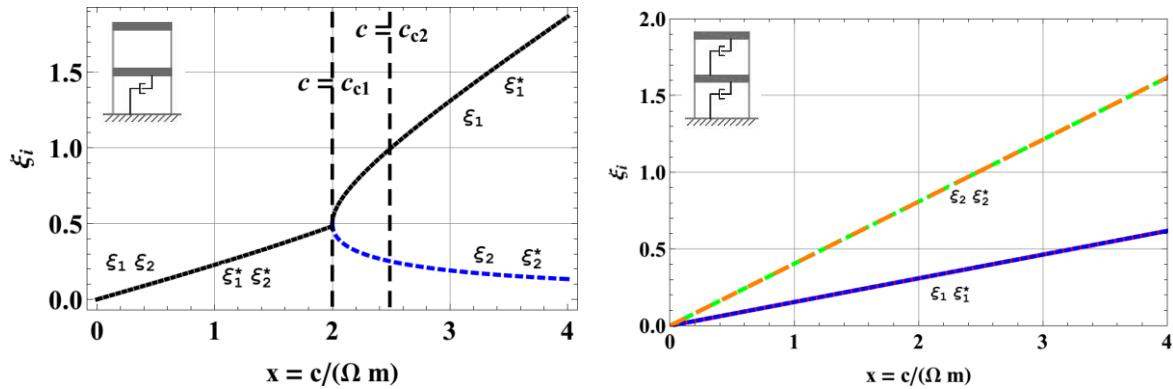
where Ω_r is an unknown frequency parameter. This parameter can be found by subtracting Eq. (26) which leads to $\Omega_r = \sqrt{\lambda_r \lambda_{r+1}}$. Similarly, the supercritical damping ratio ζ_r can be obtained by adding Eq. (26), yielding $\zeta_r = (\lambda_r + \lambda_{r+1}) / 2 \Omega_r$. When these expressions are applied to the 2-story shear building with a single damper, the frequency parameter and the damping ratio for the first mode become

$$\Omega_1 = \sqrt{(k/m)} = \Omega \tag{27a}$$

$$\xi_1 = \left(x + \sqrt{x^2 - 4} \right) / 4 \quad ; \quad c \geq c_{c2} \tag{27b}$$

Note that Eq. (27b) is equal to Eq. (25a) for the damping ratio ζ_1 in the second zone when the mode is still underdamped.

The damping ratios can be expressed in closed form for any value of c by means of Eqs. (24), (25) and (27b). The damping ratios calculated with the proposed equations are plotted in Fig. 5(a). Fig. 5(a) reveals interesting features about the damping added to the system by a single damper in the first floor. First, when the damping coefficient is less than c_{c1} (or $x < 2$), the equivalent damping ratios of the two modes are equal. When the damping coefficient c reaches the first critical damping coefficient c_{c1} , the damping of the two modes begins to diverge: the first mode damping ratio increases whereas that of the second mode decreases. The fact that the equivalent damping ratios decrease with increased damper capacity is unexpected and it has also been reported recently (Charney and McNamara 2008). When the value of c reaches c_{c2} (or $x = 2.5$), the first mode



(a) A building with single dampers at the first floor (b) A building with equal dampers in the two floors

Fig. 5 Equivalent damping ratios

damping ratio ξ_1 becomes 1, i.e., the mode becomes overdamped.

For comparison purposes, the damping ratios of a shear building with dampers with equal coefficients $c/2$ on each of the two floors (i.e., with stiffness proportional damping) are displayed in Fig. 5(b). As expected, here the damping ratios of the first and second mode also increase with the damping coefficient, but opposite to those in Fig. 5(a) they have different values. Moreover, the damping ratio of the second mode is higher than the one of the first mode and it reaches faster the critical damping ratio $\xi_i=1$. The damping ratio for $\xi_i>1$ plotted in this figure was calculated using the pair of real eigenvalues in Eq. (26).

5.1 The meaning of the frequency parameter for the overdamped case

We mentioned that for $\xi \geq 1$ the concept of equivalent natural frequency is misleading because the structural system will not exhibit oscillations when it is set in free vibrations. According to the previous results (i.e., see Fig. 5(a)) the second mode is always underdamped but the first mode becomes overdamped when $c > c_{c2}$ (i.e., $x > 2.5$). It was proposed to express the eigenvalues of the two overdamped modes in the form of Eq. (26) in terms of the damping ratio and a variable that was referred to as the frequency parameter Ω_r . It is called a “frequency” because it has the units of a circular frequency, i.e. rad/time. A physical meaning can be given to this parameter by examining the free vibration response of the damped system written in terms of real quantities, Eq. (4). This equation is valid for underdamped modes but if there is a pair of overdamped modes, say the r^{th} and $(r+1)^{\text{th}}$ modes, it can be modified as follows

$$\begin{Bmatrix} \dot{u} \\ u \end{Bmatrix} = \sum_{\substack{j=1 \\ j \neq r, r+1}}^{2n} \left(\{A_j\} \cos \omega_{d_j} t + \{B_j\} \sin \omega_{d_j} t \right) e^{-\xi_j \omega_j t} + \left(\{C_r\} \cosh \Omega_{dr} t + \{D_r\} \sinh \Omega_{dr} t \right) e^{-\xi_r \Omega_r t} \quad (28)$$

where $\Omega_r = \sqrt{\lambda_r \lambda_{r+1}}$ is the frequency parameter and $\Omega_{dr} = \Omega_r \sqrt{\xi_r^2 - 1}$ is a damped frequency parameter defined in terms of Ω_r and the damping ratio $\xi_r \geq 1$. For a shear building with one damper, the frequency parameter for $r=1$ is given by Eq. (27a).

The vectors $\{C_r\}$ and $\{D_r\}$ are defined by the pair of real eigenvectors $\{\psi\}_r$ and $\{\psi\}_{r+1}$ and the initial values of the modal coordinates associated with these two modes (Pierson *et al.* 2013).

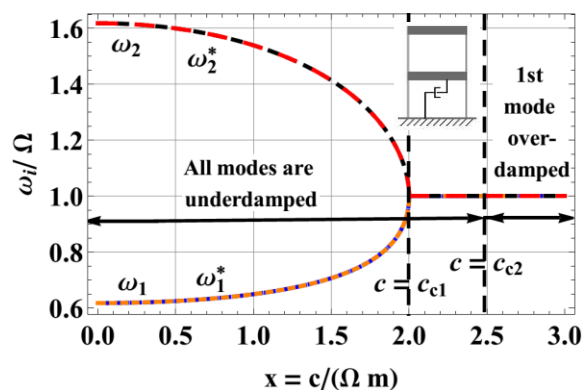


Fig. 6 Equivalent natural frequencies with underdamped and overdamped regions

According to Eq. (28), the values of the damping ratio ζ_r and the frequency parameter Ω_r specify how fast the overdamped modes tend to rest whereas Ω_{dr} in the hyperbolic sine and cosine affects the peak displacement and velocity. The overdamped modes play an important role in the structural response. They have a significant influence on the absolute acceleration and the response of the structure is underestimated when the modes are not properly considered (Chu *et al.* 2008). The plot of the equivalent natural frequencies is updated in Fig. 6 and although Ω_r is not an equivalent natural frequency, the range where $\omega_1 = \Omega_1$ was included to explain the results of the numerical examples in the following section.

6. Validation and interpretation of the equivalent natural frequency

We will verify through a numerical example the accuracy of the proposed equations that define the equivalent natural frequencies, Eqs. (17), (21), and (27a), and the equivalent damping ratios, Eqs. (24), (25) and (27b). A regular shear building with lateral stiffness coefficient $k=18,000$ kN/m (1,000 k/in) and a lumped mass $m=19,600$ kg (0.4 k.s²/in) is considered. Four values of the damping coefficient at the first floor are used: 1) less than c_{c1} ($c=594$ kN.s/m), 2) equal to c_{c1} ($c=1188$ kN.s/m), 3) between c_{c1} and c_{c2} ($c=1336$ kN.s/m), and 4) higher than c_{c2} ($c=1782$ kN.s/m).

The simulated free vibration response of this structural system was evaluated by solving the equation of motion via direct integration with the Average Acceleration Method (Humar 2012). The sampling frequency was 500 Hz ($\Delta t=0.002$ s) and the accelerations at the first and second floor were computed. From this data, the frequencies and the damping ratios were estimated using various signal processing techniques, i.e. Fourier, wavelet and Hilbert transforms (Gaviria and Montejo 2015a, b). All these procedures were implemented in Matlab (Matlab-7.14 2012). It is important to bear in mind that for the numerical simulations (the response calculations and signal processing of the response) neither the complex eigenvalues and eigenvectors, nor the equivalent natural frequencies and damping ratios were used. The objective is to compare the dynamic properties calculated using the proposed equations (i.e., those based on the state space formulation with complex quantities) with the natural frequencies and the damping ratios identified from well-established signal processing techniques.

Fig. 7(a) shows 0.5 s of the free vibration response of the first floor for the four damping coefficients. The Fourier spectra of the free vibration acceleration records are depicted in Fig 7(b).

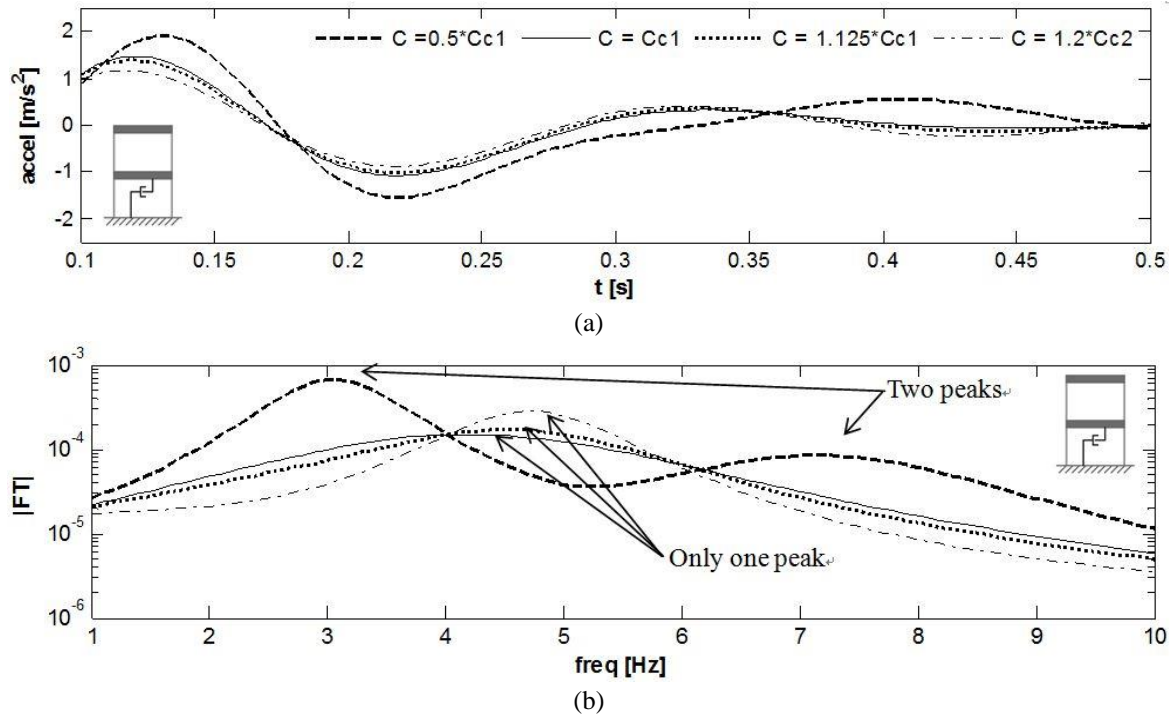


Fig. 7 (a) Free vibration responses; (b) Fourier spectra of the accelerations

Table 1 Verification of the expressions for the equivalent natural frequency and damping ratios

Case	x	ω_{eq}/Ω				ξ			
		Mode 1		Mode 2		Mode 1		Mode 2	
		Eqs.	Ident.	Eqs.	Ident.	Eqs.	Ident.	Eqs.	Ident.
$c < c_{c1}$	1.00	0.65	0.66	1.54	1.55	0.228	0.223	0.228	0.235
$c = c_{c1}$	2.00	1.00	1.00*	1.00	1.00*	0.500		0.500	
$c_{c1} < c < c_{c2}$	2.25	1.00		1.00	0.99	0.820		0.305	0.310
$c > c_{c2}$	3.00	1.00		1.00	0.99	1.309		0.191	0.189

* This value was computed using the damping ratio from Eq. (24).

It can be seen in this figure that for the first case ($c \leq c_{c1}$), there are two peaks in the Fourier spectrum, from which vibration frequencies can be extracted. On the other hand, in the other cases ($c \geq c_{c1}$) only one frequency can be identified. Also, this latter frequency has a value between those frequencies of the first case ($c \leq c_{c1}$). The foregoing observations are in agreement with the variation of the equivalent frequencies described by Eqs. (17), (21) and (27a) that were displayed in Fig. 6. Table 1 compares the identified dynamic properties using signal processing procedures (Ident) and the values calculated with the proposed equations for the equivalent natural frequencies and damping ratios (Eqs). An empty cell indicates that the signal processing methods did not identify the dynamic property. The values of the identified equivalent natural frequencies (ω_j) are computed using the identified damped frequencies and damping ratios (i.e., $\omega_j = \omega_j / \sqrt{1 - \xi_j^2}$). This table shows that the identified properties are very close to the values calculated with the proposed

equations for all the cases examined. Therefore, it is confirmed that the structure vibrates with the equivalent natural frequencies rather than the undamped natural frequencies, i.e., Eqs. (6a) and (8). The concept of equivalent natural frequency presented here could be considered in design procedures like the response spectrum analysis in FEMA 450 (2004) and ASCE 7-05 (2006).

7. Dynamic characteristics of a 2-story building with a damper in the 1st floor: a summary

The equations and figures describing the dynamic properties were presented in non-dimensional form in order to be valid for any 2-story shear building model with regular mass and stiffness distribution. From Figs. 2(a) and 2(b) we identified two damping coefficients where the dynamic behavior of the system changes; they were called the first and second critical damping coefficients. Figs. 5(a) and 6 summarize the variations of the damping ratios and equivalent natural frequencies with the dimensionless damping coefficient. A highlight of the findings is listed next:

- For values of the damping coefficient less than the first critical damping coefficient ($c < c_{c1} = 2\sqrt{km}$), the equivalent natural frequencies are a function of c , k , and m (Eq. (21)). Also, the two modes share the same damping ratios for the entire region. Therefore, the building with one damper can be more effective than that with one damper per floor because the former dissipates the same energy in all the modes. Similar results have been reported in a particular analysis of the seismic retrofit of a historic concrete building where viscous dampers were only installed in the first floor (Miyamoto *et al.* 2003). Lewandowski (2008) also recommended that the dampers in shear building models must be located in a few appropriate stories. Additionally, for economic reasons it is usually recommended to limit the damping ratios achieved with viscous fluid dampers to 25% (Lee and Taylor 2001). However, since it was shown that a single damper is sufficient to obtain higher damping levels, this limitation may be rescinded.

- An interesting situation occurs if the damping coefficient is equal to the first critical damping coefficient: the structure vibrates as a single dof system because their equivalent natural frequency and equivalent damping ratios for both modes become equal (the modes are fused).

- Between the first and second critical damping coefficient ($c_{c1} < c < c_{c2}$) the equivalent natural frequencies of both modes remains equal to Ω , i.e., the frequency of a single dof system with the mass m and lateral stiffness k of one floor (Eq. (9)). However, the two modes contribute to the structural response because their associated equivalent damping ratios are different (Fig. 5(a)). The effectiveness of the damper is reduced in this zone because the damping ratio of the second mode decreases as the damping coefficient increases (Eq. (25b)).

- When the coefficient c becomes equal to c_{c2} , the equivalent damping ratio of the first mode turns >1 and the first mode becomes overdamped (Fig. 5(a)). Thus, the first equivalent natural frequency dies out and the response is mostly due to the contribution of the second mode (see Fig 7(b) and Table 1).

8. Numerical example of seismic response

Although it is not the main objective of paper, in order to present some implications of the proposed formulation we will examine the variation with the damping coefficient of the seismic response of the sample 2-story building. The bare structure has an inherent damping ratio of 0.02 for all the modes. Five accelerograms representing ground motions with different frequency

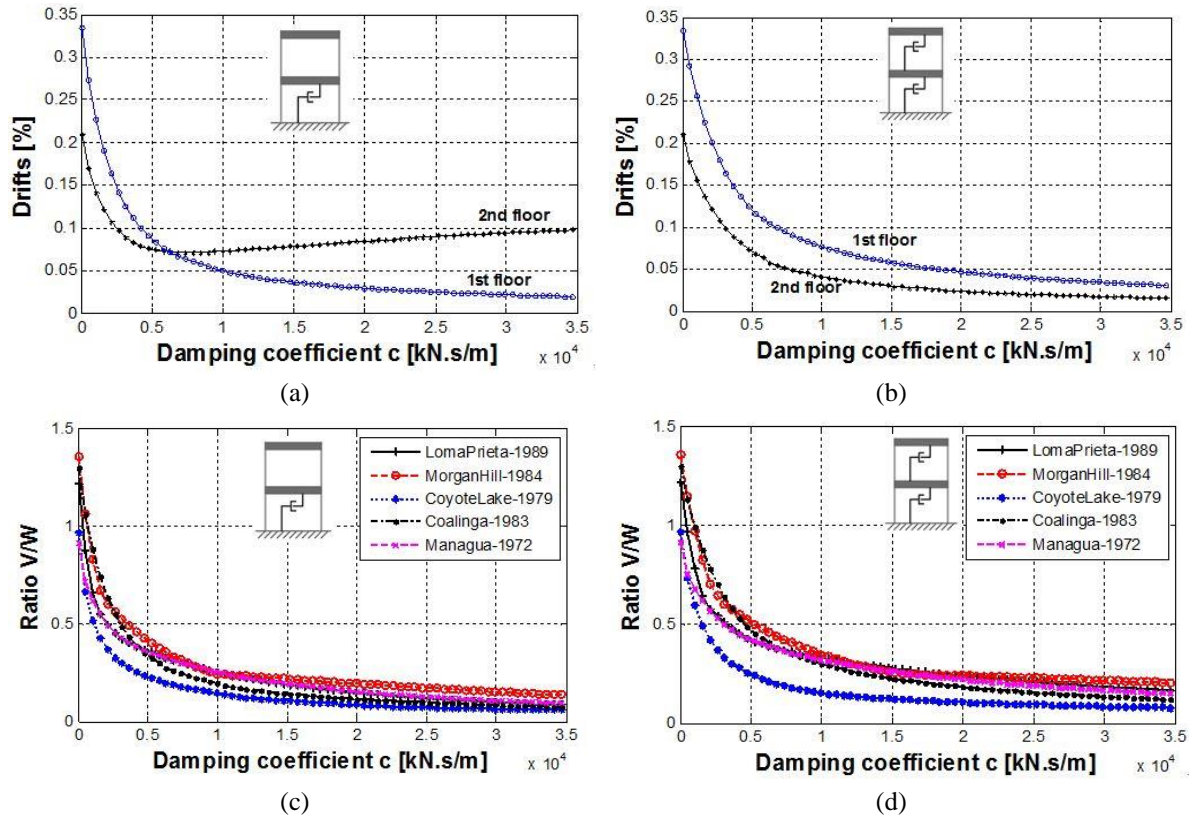


Fig. 8 Maximum drifts for the Coalinga earthquake: (a) building with one damper; (b) with two equal dampers. Variation of ratios V/W for five earthquakes: (c) building with one damper; (d) with two equal dampers

content, from narrow band to broad band signals were used. The records were obtained from the Next Generation Attenuation of Ground Motions (NGA) project (PEER 2006). To limit the number of variables all accelerograms were scaled to a PGA of 0.3g. The peak drift variations of the two building levels exhibit an interesting behavior. Fig. 8(a) presents the case for the 1983 Coalinga earthquake: note that once the damping coefficient exceeds a certain value, the drift of the second floor starts to increase slowly and for other earthquakes is almost constant. There is also a point ($c=6,157 \text{ kN.s/m} = 35 \text{ k.s/in}$ in this case) where the two drifts are identical. This particular value of c depends on the earthquake and its average for all the ground motions considered is $8,400 \text{ kN.s/m}$ (48 k.s/in). This damping coefficient is close to the first critical damping coefficient $c_{c1} = 2\sqrt{km} = 7,005 \text{ kN.s/m}$ (40 k.s/in) beyond which the second mode damping ratio starts to decrease as the damping coefficient c increases (see Fig. 5(a)). Therefore, for this configuration it is recommended to use a damper with a coefficient $c \leq c_{c1}$.

The ratio between the maximum base shear and the total weight of the building V/W (known as the seismic coefficient) is plotted in Fig. 8(c) as a function of the damping coefficient for the five earthquakes. Note that the pattern of variation is the same for all the ground motions. When the damping coefficient is equal to c_{c1} , the average ratio V/W for the 2-story building with one damper is 0.280 whereas when $c=0$, it is 1.149.

It is noteworthy to compare the seismic response of the same 2-story building but with equal dampers in all floors. The sum of the two damping coefficients is taken equal to the shear building with one damper. The maximum drifts as a function of the damping coefficient for the 1983 Coalinga record are displayed in Fig. 8(b): note that the drifts of the two floors always decrease as the damping coefficient increases. Fig. 8(d) shows the ratios V/W as a function of the damping coefficient for the five ground motions. The response of the building with a single damper is somewhat smaller than the one with two dampers. This could be to the fact that when the damping coefficient is smaller than the first critical value, the two modes of the building with one damper have the same damping ratio.

9. Conclusions

A procedure to obtain closed-form expressions for the dynamic properties of structural systems with a non-proportional damping matrix was presented. The procedure is applied to the simple case of a 2-dof shear building model with a single damper in the first floor. The dynamic properties, i.e. the equivalent natural frequencies and damping ratios, were obtained in closed form as a function of the stiffness and mass coefficients of the structure and the damper coefficient. These equations show that the expressions available in the literature to calculate the equivalent natural frequency and damping ratio are not applicable for systems with dampers placed such that the damping matrix becomes arbitrary. New formulas were provided to circumvent the problem, which also account for the case of overdamped systems. It is shown that the damper not only contributes to the energy dissipation but it also changes one of the most important dynamic characteristics of system: its vibration frequencies.

An insight into the meaning of the equivalent natural frequency is provided via the numerical simulation of the free vibration response of a building. It is shown that when the structure with dampers is set in free vibration, it oscillates with the equivalent natural frequency and not with the damped natural frequency.

The variation of the equivalent natural frequencies and damping ratios with a non-dimensional parameter that considers the damping coefficient, the mass and stiffness of the building model is studied. Depending on the value of the damping coefficient, three distinct zones can be observed, separated by two values referred to as the first and second critical damping coefficient. Before the damping coefficient reaches the first critical coefficient, all the modes share the same damping ratio. From that point on, the damping ratio of the first mode increases whereas the one of the second mode decreases.

The response of the damped building to several earthquakes with different characteristics was examined. It was found that not every response quantity always decreases as dampers with larger coefficients are used. This is the case of the maximum drift at the second level of the building, which reaches a minimum and then increases or remains constant (depending on the earthquake). Therefore, for this structural system it is recommended to select a damper with a coefficient smaller than the first critical value.

All the formulas and graphs of the dynamic properties were presented in non-dimensional form so that they are valid for any 2-story shear building model with uniform mass and stiffness. Similar to the design of a based isolated system, one can define target values for the equivalent natural frequencies and damping ratios, and then use graphs such as those in Figs. 5(a) and 6 to determine the required damping coefficient. It may not be possible to obtain closed form expressions for the

equivalent frequency and damping ratios of systems with more than 2 dof with dampers in a non-proportional arrangement because there is no general algebraic solution to polynomial equations of fifth degree or higher (Jacobson 2012). However, the procedure presented is valid for other mdof systems for which a numerical evaluation of the structures with dampers can be used to build dimensionless curves similar to Figs. 5(a) and 6.

Because the formulas presented are limited to a simple structural system, it is not presumed that they will have direct applications, nor they were intended for that purpose. However, the formulation can be useful to understand unexpected results that may occur in similar cases, e.g. when a single damper is placed in a regular structure. For instance, it can help to explain why the damping ratios of several modes become equal, why the damping ratio of a certain mode decreases as larger dampers are used (Charney and McNamara 2008), or why the higher modes have an important contribution to the seismic behavior of a building with dampers (Chu *et al.* 2008).

The equivalent natural frequency can be incorporated in design procedures for structures with dampers, such as the response spectrum analysis presented in FEMA 450 (2004) and Chapter 18 of ASCE 7-05 (2006). As previously reported (Symans *et al.* 2008), the results presented here corroborate that the introduction of energy dissipation devices in a structural system introduces several analysis problems that must be considered but which are not directly incorporated in design codes and guides.

References

- Adhikari, S. (2011), "An iterative approach for nonproportionally damped systems", *Mech. Res. Commun.*, **38**(3), 226-230.
- Antsaklis, P.J. and Michel, A.N. (2007), *Linear Systems*, Birkhauser Boston, New York, NY, US.
- ASCE 7-05 (2006), *Minimum Design Loads for Buildings and Other Structures*, ASCE, Reston, Virginia.
- Constantinou, M.C. and Symans, M.D. (1993), "Experimental study of seismic response of buildings with supplemental fluid dampers", *Struct. Des. Tall Build.*, **2**(2), 93-132.
- Charney, F. and McNamara, R. (2008), "Comparison of methods for computing equivalent viscous damping ratios of structures with added viscous damping", *J. Struct. Eng.*, **134**(1), 32-44.
- Cheng, F.Y., Jiang, H. and Lou, K. (2010), *Smart Structures: Innovative Systems for Seismic Response Control*, CRC Press, Boca Raton, Florida, US.
- Chu, Y.L., Song, J. and Lee, G.C. (2008), "Modal analysis of arbitrarily damped three-dimensional linear structures subjected to seismic excitations", Technical Report MCEER-09-0001, SUNY, Buffalo, NY.
- FEMA 450 (2004), *Recommended Provisions for Seismic Regulations for New Buildings and Other Structures*, Federal Emergency Management Agency, Washington DC.
- Gaviria, C.A. and Montejo, L.A. (2015a), "Optimal wavelet parameters for system identification", *Mech. Syst. Signal Pr.* (under Review)
- Gaviria, C.A. and Montejo, L.A. (2015b), "Output-only identification of modal and physical properties using free vibration response", *Earthq. Eng. Eng. Vib.* (in Press)
- Humar, J.L. (2012), *Dynamics of Structures*, Taylor & Francis Group, London, UK.
- Jacobson, N. (2012), *Basic Algebra I*, Dover Publications, Mineola, NY, US.
- Krenk, S. (2005), "Frequency analysis of the tuned mass damper", *J. Appl. Mech.*, **72**(6), 936-942.
- Lee, D. and Taylor, D.P. (2001), "Viscous damper development and future trends", *Struct. Des. Tall Build.*, **10**(5), 311-320.
- Lewandowski, R. (2008), "Optimization of the location and damping constants of viscous dampers", *Ninth International Conference on Computational Structures Technology*, Athens, September.
- Lewandowski, R., Bartkowiak, A. and Maciejewski, H. (2012), "Dynamic analysis of frames with viscoelastic dampers: a comparison of damper models", *Struct. Eng. Mech.*, **41**(1), 113-137.

- Lewandowski, R. and Pawlak, Z. (2011), "Dynamic analysis of frames with viscoelastic dampers modelled by rheological models with fractional derivatives", *J. Sound Vib.*, **330**(5), 923-936.
- Lin, J.L., Bui, M.T. and Tsai, K.C. (2013), "An Energy-based approach to the generalized optimal locations of viscous dampers in two-way asymmetrical buildings", *Earthq. Spectra*, **30**(2), 867-889.
- Ma, F., Imam, A. and Morzfeld, M. (2009), "The decoupling of damped linear systems in oscillatory free vibration", *J. Sound Vib.*, **324**(1-2), 408-428.
- Ma, F., Morzfeld, M. and Imam, A. (2010), "The decoupling of damped linear systems in free or forced vibration". *J. Sound Vib.*, **329**(15), 3182-3202.
- Matlab-7.14 (2012), The MathWorks, Inc, Natick, Massachusetts.
- Mayer, R.L. and Naguib, W.I. (2005), "Comparative seismic performance of four structural systems and assessment of recent AISC BRB test requirements", *74th Annual Convention of Structural Engineers Association of California*, San Diego, California.
- Miyamoto, H., Determan, L., Gilani, A. and Hanson, R. (2003), "Seismic rehabilitation of historic concrete structure with fluid viscoelastic dampers", *72nd Annual Structural Engineers Association of California Convention*, Sacramento, September.
- Miyamoto, H.K. and Gilani, A. (2008), "Design of a new steel-framed building using ASCE 7 damper provisions", *ASCE Structures Congress*, Vancouver, April.
- Morzfeld, M., Ajavakom, N. and Ma, F. (2009), "Diagonal dominance of damping and the decoupling approximation in linear vibratory systems", *J. Sound Vib.*, **320**(1-2), 406-420.
- NGA database (2006), *Next Generation Attenuation of Ground Motions*. Pacific Earthquake Engineering Research Center, University of California, Berkeley.
- Occhiuzzi, A. (2009), "Additional viscous dampers for civil structures: Analysis of design methods based on effective evaluation of modal damping ratios", *Eng. Struct.*, **31**(5), 1093-1101.
- Pawlak, Z. and Lewandowski R. (2013), "The continuation method for the eigenvalue problem of structures with viscoelastic dampers", *Comput. Struct.*, **125**, 53-61.
- Pawlak, Z. and Lewandowski, R. (2014), "The qualitative differences in dynamic characteristics of structures with classical and fractional dampers", *Proceedings of the Twelfth International Conference on Computational Structures Technology*, Stirlingshire, Scotland.
- Pettinga, J., Oliver, S. and Kelly, T. (2013), "A design office approach to supplemental damping using fluid viscous dampers", *Steel Innovations Conference*, Christchurch, New Zealand, February.
- Pierson, H., Brevick, J. and Hubbard, K. (2013), "The effect of discrete viscous damping on the transverse vibration of beams", *J. Sound Vib.*, **332**(18), 4045-4053.
- Soong, T.T. and Dargush, G.F. (1997), *Passive Energy Dissipation Systems in Structural Engineering*, John Wiley & Sons Ltd, Baffins Lane Chichester, UK.
- Suarez, L.E. and Gaviria, C.A. (2014) "Equivalent frequencies and damping ratios of buildings with viscous fluid dampers: A closed form formulation", *10th US National Conference on Earthquake Engineering*, Anchorage, Alaska.
- Symans, M., Charney, F., Whittaker, A., Constantinou, M., Kircher, C., Johnson, M. and McNamara, R. (2008), "Energy dissipation systems for seismic applications: Current practice and recent developments", *J. Struct. Eng.*, **134**(1), 3-21.
- Trombetti, T. and Silvestri, S. (2006), "On the modal damping ratios of shear-type structures equipped with Rayleigh damping systems", *J. Sound Vib.*, **292**(1-2), 21-58.
- Trombetti, T. and Silvestri, S. (2007), "Novel schemes for inserting seismic dampers in shear-type systems based upon the mass proportional component of the Rayleigh damping matrix", *J. Sound Vib.*, **302**(3), 486-526.
- Whittle, J., Williams, M., Karavasilis, T.L. and Blakeborough, A. (2012), "A comparison of viscous damper placement methods for improving seismic building design", *J. Earthq. Eng.*, **16**(4), 540-560.
- Wolfram Mathematica 9.0 (2012), Wolfram Research Inc, Champaign, Illinois, USA.